Stem Cell Rev and Rep
DOI 10.1007/s12015-013-9483-y

Donor Mesenchymal Stromal Cells (MSCs) Undergo Variable Cardiac Reprogramming in Vivo and Predominantly Co-Express Cardiac and Stromal Determinants after Experimental Acute Myocardial Infarction

Gustavo Yannarelli · James N. Tsoporis · Jean-Francois Desjardins · Xing Hua Wang · Ali Pourdjabbar · Sowmya Viswanathan · Thomas G. Parker · Armand Keating

Abstract We previously showed the emergence of predominantly non-fused murine cells co-expressing cardiac and stromal determinants in co-cultures of murine mesenchymal stromal cells (MSCs) and rat embryonic cardiomyocytes. To determine whether a similar phenotype is detectable in vivo in ischemic myocardium, we infused green fluorescence protein (GFP)-marked MSCs intravenously into wild-type mice in an acute myocardial infarction (AMI) model generated by ischemia/reperfusion (I/R) or fixed coronary artery ligation. We found that infused GFP+ cells were confined strictly to ischemic areas and represented approximately 10 % of total cellularity. We showed that over 60 % of the cells co-expressed collagen type IV and troponin T or myosin heavy chain, characteristic of MSCs and cardiomyocytes, respectively, and were CD45(-). Nonetheless, up to 25 % of the GFP+ donor cells expressed one of two cardiomyocyte markers, either myosin heavy chain or troponin T, in the absence of MSC determinants. We also observed a marked reduction in OCT4 expression in MSCs pre-infusion compared with those lodged in the myocardium, suggesting reduced stem cell properties. Despite the low frequency of lodged donor MSCs, left-ventricular end-diastolic pressure was significantly better in experimental versus saline animals for both AMI (12.10± 1.81 vs. 20.50±1.53 mmHg, $p<0.001$) and I/R models (8.75 ±2.95 vs. 17.53±3.85 mmHg, $p=0.004$) when measured 21 days after MSC infusion and is consistent with a paracrine effect. Our data indicate that donor MSCs undergo variable degrees of cardiomyocyte reprogramming with the majority co-expressing cardiomyocyte and stromal markers. Further studies are needed to elucidate the factors mediating the extent of cardiomyocyte reprogramming and importance of the cellular changes on tissue repair.

Keywords Mesenchymal stromal cells · Cardiomyocyte reprograming · Acute myocardial infarction

Introduction

Cardiovascular disease is a leading cause of death globally [1]. Cell-based therapies with bone marrow-derived mesenchymal stromal cells (BM-MSCs) appear to have therapeutic potential [2]. BM-MSCs can induce angiogenesis, inhibit cardiomyocyte apoptosis, and improve left ventricular function in acute myocardial infarction (AMI) models [3]. The beneficial effects were originally attributed to the ability of MSCs to differentiate into cardiomyocytes, both in vitro and in vivo [4–8]. However, BM-MSC reprogramming towards the cardiac lineage is controversial mainly because of the use of

Gustavo Yannarelli and James N. Tsoporis contributed equally to this work.

Electronic supplementary material The online version of this article (doi:10.1007/s12015-013-9483-y) contains supplementary material, which is available to authorized users.

G. Yannarelli · X. H. Wang · S. Viswanathan · A. Keating (✉)
Cell Therapy Program, Princess Margaret Hospital, University Health Network, University of Toronto, 610 University Ave, Suite 5-303, Toronto, ON, Canada M5G 2M9
e-mail: armand.keating@uhn.ca

J. N. Tsoporis · J.-F. Desjardins · A. Pourdjabbar · T. G. Parker
Division of Cardiology, Department of Medicine, Keenan Research Centre, Li Ka Shing Knowledge Institute, St. Michael's Hospital, Toronto, ON, Canada

Published online: 28 November 2013

heterogeneous hematopoietic cell populations and significant differences in the frequency and origin of the cells lodging in ischemic myocardium [9]. In addition, as only limited engraftment of MSCs has ever been reported [10], it is not widely believed that MSCs actually differentiate into cardiac cells to effect contractile recovery, although this theory has not been fully discounted. Indeed, various reports failed to demonstrate MSCs differentiation into functional cardiomyocytes and concluded that indirect mechanisms such as cytokine release and angiogenesis mediate the cardiac repair [11–17]. We previously showed that BM-derived murine MSCs acquire cardiac markers but retain MSCs properties when co-cultured with rat embryonic cardiomyocytes [18]. Thus, our data may explain some of the controversies in the literature and suggest that although BM-MSCs demonstrate cell lineage plasticity, their differentiation into cardiomyocytes is partial in vitro, supporting the paracrine hypothesis. It has been shown that the release of soluble growth factors and cytokines is influenced by the developmental status and properties of the MSCs [19]. Moreover, cardiac lineage pre-specification enhances the therapeutic benefit of human BM-MSCs in a murine model of chronic myocardial infarction [20–24]. These data suggest that priming towards the cardiac lineage may be required to engender cardiac repair. However, the multipotent properties of BM-MSCs may be different in vivo and the frequency and extent of this partial differentiation need to be assessed.

The aim of this study was to undertake a quantitative determination of whether partially differentiated BM-MSCs are detectable in vivo in ischemic myocardium. To this end, we employed an intrinsically marked, well-characterized stromal cell population administered intravenously after ischemia-reperfusion AMI versus AMI alone in a murine model. Twenty-one days after BM-MSC infusion, we assessed cardiac hemodynamic function and analyzed the extent of cardiomyocyte differentiation of the lodged donor cells using anti-GFP antibodies and a panel of monoclonal antibodies against cardiomyocyte and MSC determinants. Here, we show that the majority of donor BM-MSCs in the ischemic area had acquired at least one cardiac marker but retained stromal cell characteristics. In addition, we found that the expression of the pluripotency transcription factor OCT4 significantly decreased in BM-MSCs after lodgement in the heart, consistent with the acquisition of a more differentiated phenotype. Nonetheless, we also observed a minor population that expressed cardiac markers but lacked stromal determinants, suggesting the presence of more extensive cardiac reprogramming of the donor BM-MSCs.

Materials and Methods

Mice

Transgenic B5/GFP mice, which have an ICR strain background, were crossed onto a Balb/cByJ background by eight successive mating with Balb/cByJ mice (Jackson Laboratory, Bar Harbor, ME). The GFP-Balb/c crossbred mice generated GFP(+) and GFP(-) offspring in the expected Mendelian ratios. The mice were housed at the Ontario Cancer Institute Animal Resource Center, according to institutionally approved protocols.

Isolation and Characterization of Bone Marrow-Derived MSCs

Bone marrow cells were collected from the femur and tibia of individual GFP-Balb/c male mice and stromal cells generated according to our established method [25]. Briefly, 4–5$\times 10^7$ mononuclear cells per mouse were collected, plated at 0.5−1.0$\times 10^5$ cells per cm^2 and cultured in α-medium (Gibco BRL, Burlington, ON, Canada) with 10 % horse serum, 10 % fetal bovine serum (HyClone Laboratories, Logan, UT, USA), 10^{-6} M hydrocortisone (Sigma, St Louis, MO, USA), 1 % L-glutamine, and antibiotics (Gibco BRL). The cells were incubated at 37 °C in a humidified incubator containing 5 % CO_2 and were serially passaged when they reached near confluence (every 5–7 days) until fourth passage MSCs were obtained. BM-MSCs were characterized by flow cytometry using antibodies against CD44 (APC-labelled, eBioscience), CD73 (PE-labelled, BD Pharmingen), CD90 (PE-labelled, Abcam), CD105 (PE-labelled, eBioscience), CD45 (APC-labelled, BD Pharmingen), CD14 (PE-labelled, eBioscience), CD31 (PE-labelled, eBioscience) and CD34 (PE-labelled, BD Pharmingen). For each marker, the pellet (2×10^4 cells) was re-suspended in 100 μl of PBS and stained by adding 2 μl of the corresponding antibody (1:50 dilution) for 30 min. After washing, fluorescence was evaluated in a Beckman-Coulter Cytomics FC-500 and data analyzed using FlowJo software (TreeStar). To determine MSCs multilineage differentiation potential, cells were plated in 12-well plates at a density of 1×10^4 cells/cm^2. For adipogenic differentiation, cells were cultured in DMEM medium supplemented with 10 % FBS, 0.5 mM 3-isobutyl-1-methylxanthine, 60 μM indomethacin, 10 μg/ml insulin, and 1 μM dexamethasone with media replaced every 3 days. At 10–12 days of adipogenic induction, cells were washed twice with PBS, fixed with 4 % paraformaldehyde and stained with 0.5 % oil red O to visualize lipid droplets. For osteogenic differentiation, cells were cultured in DMEM medium supplemented with 10 % FBS, 10 mM β-glycerophosphate, 50 μM ascorbic acid-2-phosphate, and 0.1 μM dexamethasone with media replaced every 3 days. After 21 days, cells were rinsed with calcium and phosphate-free saline solution, and fixed with

ice-cold 70 % ethanol for 1 h. After a brief wash with water, the cells were stained for 10 min with 40 mM Alizarin Red S solution (pH 4.2) to visualize mineralized bone matrix.

Myocardial Ischemia and Reperfusion Model

Twelve-week-old Balb/c mice were anesthetized using a mixture of ketamine (40 mg/kg) and pentobarbital sodium (33 mg/kg) via intraperitoneal injection. Endotracheal intubation was performed in the supine position under direct laryngoscopy using a blunt-ended 22-gauge catheter and the mice were ventilated with a small animal respirator (Harvard Apparatus; tidal volume=1.0 ml, rate=120 breaths/min). Proper intubation was confirmed by observation of chest expansion and retraction during ventilated breaths. During the operation, the animals were kept warm with heat lamps. The chest was opened by a horizontal incision made in the muscle between the fourth and fifth ribs exposing the heart. The pericardial sac was removed and ischemia was achieved by ligating the anterior descending branch of the left coronary artery (LAD) with a 7-0 silk suture. A 1-mm section of PE-10 tubing was placed on top of the LAD, 1 to 3 mm from the tip of the normally positioned left atrium. Regional ischemia was confirmed by visual inspection of the occluded distal myocardium. For the ischemia-reperfusion experiments, after occlusion for 90 min, the ligature and PE-10 tubing were removed to restore perfusion. Blood flow was confirmed by visualization of a return of red color to the previously pale region of myocardium. A 7-0 silk suture was used to close the chest. Finally, the endotracheal tube was withdrawn and the animal was given the analgesic butorphanol tartrate (0.1 mg/kg) and kept warm by placing the cage on a 37 °C warm plate for 1 to 2 h. The procedure for sham-operated mice was the same, except that the LAD coronary artery was not ligated.

BM-MSCs Infusion

Fourth passage BM-MSC from GFP-Balb/c mice (5×10^5 cells/0.2 ml/mouse) were injected intravenously into the tail vein of Balb/c mice 3–4 h following experimental AMI with and without ischemia/reperfusion. An injection of saline was used in the control animals. See supporting information Figure S1 for a schematic diagram of the study design.

Hemodynamic Studies

Mice were anesthetized with an intra-peritoneal injection of a mixture of ketamine 62.5 mg/kg (Bimeda-MTC Animal Health Inc., Cambridge ON), and xylazine 12.5 mg/kg (Bayer Canada, Etobicoke, ON) 21 days after instrumentation. Heart rate, systolic and diastolic arterial pressures were measured using a Millar micro-tip catheter transducer (SPR-671, Millar Instruments Inc, Houston, TX), inserted into the right carotid artery as previously described [26]. The catheter was then advanced into the left ventricle (LV) under the guidance of the pressure signal for the measurement of LV pressure, and the maximum rate of pressure rise (+dP/dt) and decline (-dP/dt). All data were acquired and analyzed through the Digi-Med Blood Pressure Analyzer (Louisville, KY) according to the manufacturer instructions. Mean Arterial pressure (MAP) was calculated using the following equation: MAP (mm Hg)=1/3(SP - DP)+DP, systolic pressure (SP), diastolic pressure (DP). Once the hemodynamic measurements were completed, the mice were euthanized and the heart and lungs were excised and weighed.

Echocardiographic Assessment of Cardiac Hypertrophy and Function

Echocardiography imaging, with a 12-mHz probe (Hewlett Packard Sonos 5500, Philips, Ultrasound, Bothell), was performed as described previously [26]. LV internal diameters at end diastole (LVIDd) and end systole (LVIDs) were measured on the two-dimensional image from M-mode tracings at the level of the papillary muscles and recorded as the consensus of a signal observed blinded to the identity of the mice. For each measurement, consecutive cardiac cycles were measured and then averaged. Fractional shortening (FS) in percent was calculated as (LVIDd - LVIDs)/LVIDd×100, and ejection fraction (EF) as ($LVIDd^3$ - $LVIDs^3$)/$LVIDd^3$.

Harvesting of Cardiac Tissue

On day 21 after LAD ligation, mice were euthanized to harvest lung tissue as well as cardiac tissue for measurement of LV and RV weights. Cardiac tissue was also fixed and stained with hematoxylin and eosin and examined microscopically [27].

Immunostaining

For immunostaining, three adjacent sections from cryo- and paraffin blocks of myocardium were cut and placed on separate slides. The middle section was stained with propidium iodide and the adjacent sections were processed for immunostaining. In all cases, the specificity of the immunolocalization was determined by using a non-immune antibody of the same isotype as the primary antibody against each specific protein.

For GFP immunostaining, the sections were incubated for 60 min with a rabbit polyclonal anti-GFP antibody (Molecular Probes) (diluted 1:10), followed by donkey anti-rabbit IgG linked with the Alexa Fluor® 488 (Santa Cruz Biotechnology) (diluted 1:50) for 60 min. For GFP and cardiac troponin T-C double staining, the sections were incubated for 60 min with a rabbit polyclonal anti-GFP antibody (Molecular Probes) (diluted 1:10) and with a goat polyclonal anti-cardiac-troponin T-C (C-19) (diluted 1:20) (Santa Cruz Biotechnology); in this case, an Alexa Fluor® 633 conjugated donkey anti-goat

antibody (Molecular Probes) was applied first, followed by the Alexa Fluor® 488 donkey anti-rabbit IgG. For GFP and OCT4 double staining, the sections were incubated for 60 min with a goat polyclonal anti-GFP-linked FITC antibody (Abcam) (diluted 1:100) and with a rabbit polyclonal anti-Oct4 antibody (Abcam) (diluted 1:250). The secondary antibody used was a donkey anti-rabbit Alexa Fluor® 594 (Molecular Probes). Before examination with confocal laser scanning microscopy (ZEISS, Axioplan 2 upright microscope with LSM 510 laser scanning module and Axiovision program), the specimens were rinsed with PBS and mounted in FluorSaveTM Reagent (CALBIOCHEM®). The Alexa Fluor® 488, 594 and 633 were observed using a FITC 488 filter, a Texas Red filter, and a Cy5 filter, respectively. Nuclei were stained with propidium iodide, 10 μg/ml (Sigma).

Immunostaining of collagen IV, myosin heavy chain (MHC), CD45R, CD11b, Gr-1 was performed on the frozen sections as follows: for collagen type IV, a rabbit anti-mouse collagen type IV (BIODESIGN) was used and the second antibody was an Alexa Fluor® 555 conjugated anti-rabbit IgG (Molecular Probes). Murine monoclonal antibodies were employed against myosin heavy chain (MHC), CD45R, CD11b and Gr-1 (BD Biosciences). The M.O.M.TM Kit (Vector Laboratories, Inc.) was used to decrease background staining from mouse IgG. MF20 (Developmental Studies Hybridoma Bank, Iowa City, IA) an anti-sarcomeric myosin antibody (working dilution 1:50) was used to identify cells or bodies of cardiac origin. The second antibody was an anti-mouse IgG linked with Alexa Fluor® 555. To detect CD45R, CD11b and Gr-1, the respective biotin-anti-mouse antibodies (BD Biosciences) and streptavidin Alexa Fluor® 555 conjugate were used. Fluorescence imaging was performed with ZEISS confocal microscope. GFP were observed by using a FITC 488 filter and Alexa Fluor® 555 was observed with a Cy3 filter.

For GFP, troponin T and collagen IV triple staining, GFP was detected with a rabbit polyclonal anti-GFP antibody (Molecular Probes) (diluted 1:10) and the second antibody was a donkey anti-rabbit IgG-linked Alexa Fluor®488 (Molecular Probes). A monoclonal antibody to troponin T (cardiac) (BIODESIGN) was used and the second antibody was a donkey anti-mouse IgG linked Alexa Fluor® 555 (Molecular Probes). The antibody for collagen type IV was a goat polyclonal anti-collagen type IV (BIODESIGN) while the second antibody was a donkey anti-goat IgG linked Alexa Fluor® 633 (Molecular Probes). To assess the frequency of GFP(+)/total cells, TnTc(+), GFP(+)/GFP(+), collagen type IV(+), GFP(+)/GFP(+), TnTc(+), collagen type IV(+), GFP(+)/GFP(+), total cell numbers were obtained by DAPI staining of all nuclei. For GFP, myosin heavy chain and collagen type IV triple staining, GFP and collagen type IV detection was the same as above. The myosin heavy chain was detected with a murine monoclonal antibody (MF-20) and the second antibody was a donkey anti-mouse IgG linked Alexa Fluor® 555 (Molecular Probes). In both cases, the frequency of each determinant was calculated by enumeration of GFP+ cells in the infarct zones from 5 animals receiving BM-MSCs (6 sections per animal).

For OCT4 staining of Balb/c BM-MSCs, cells in primary cultures were fixed in 4 % paraformaldehyde/PBS for 10 min, permeabilized with 0.2 % Triton X-100 in PBS for 10 min, and then blocked with 5 % FBS/PBS for 1 h. Cells were incubated overnight at 4 °C with primary antibodies against OCT4 (Abcam) (diluted 1:250). The second antibody was a donkey anti-rabbit IgG linked Alexa Fluor® 594 (Molecular Probes) (diluted 1:250). Slides were mounted with an antifade DAPI reagent (ProLong Gold, Invitrogen).

Reverse Transcription–PCR (RT-PCR)

Total RNA was extracted from cells by use of Trizol reagent (Invitrogen) as described by the manufacturer. One microgram was reverse transcribed into cDNA using random primers and MultiScribe RT (High-Capacity cDNA Reverse Transcription Kit, Applied Biosystems). Primers 5′-CAATGCCGTGAAGT TGGAG-3′ and 5′-CCAAGGTGATCCTCTTCTGC-3′ were designed near an exon-exon boundary to specifically amplify the OCT4 cDNA. Primers for GAPDH (sense primer, 5′-ATGGTGAAGGTCGGTGTGA-3′; antisense primer, 5′-CTCCACTTTGCCACTGCAA-3′) were used as an internal control. PCR reactions were carried out using Taq DNA polymerase (Invitrogen) and the following cycling conditions: 94 °C for 45 s, then 35 cycles at 94 °C for 15 s, 58 °C for 30 s, and 72 °C for 30 s, and then a final step of 72 °C for 7 min. The amplified transcripts were visualized on 2 % agarose gels with the use of ethidium bromide. Specific amplification products were observed and their identities confirmed by automatic DNA sequencing. This is particularly important as detection of OCT4 expression by RT-PCR could generate false positive results by pseudogene transcripts [28].

Western Blotting

Total cellular protein extracts were prepared as described by Maniatis et al. [29]. To separate cytoplasmic and nuclear fractions, cells were resuspended in lysis buffer (50 mM Tris–HCl, 1 % Triton X-100, 137.5 mM NaCl, 10 % Glycerol, 1 mM Na_3VO_4, 100 μg/ml PMSF, 1 μg/ml aprotinin, 1 μg/ml leupeptin), lysates were centrifuged and the supernatant was collected. The nuclear pellet was separately resuspended in the same lysis buffer containing 0.2 % SDS and briefly sonicated. Protein concentrations were determined using the micromethod of Bradford (Bio-Rad). The clear lysates (60 μg for total protein and citoplasmic fraction, and 20 μg for nuclear fraction) were separated on a 10 % SDS-PAGE gel, and transferred to a HyBlot CL film (Denville Scientific). The

membranes were hybridized overnight at 4 °C with the antibody anti-OCT4 (1:800, ab19857, Abcam) or anti-β-tubulin (1:1000, ab6161, Abcam) as internal protein loading control. Detection was made with ECL reagent (Amersham Pharmacia Biotech) according to the manufacturer's instructions.

Statistical Analysis

Continuous variables were expressed as mean ± SD. The unpaired Student *t* test was used to evaluate statistical significance in the expression of OCT4 before the infusion and after lodgment of MSCs in the ischemic area. One-way analysis of variance with the post hoc Tukey test was used for intergroup comparisons in the AMI and I/R model. A probability value< 0.05 was considered statistically significant.

Results

Characterization of GFP-Balb/c Bone Marrow-Derived MSCs

First, we characterized the cell population isolated from the bone marrow of GFP-Balb/c mice by immunophenotyping using flow cytometry (Fig. 1a). BM-MSCs expressed the

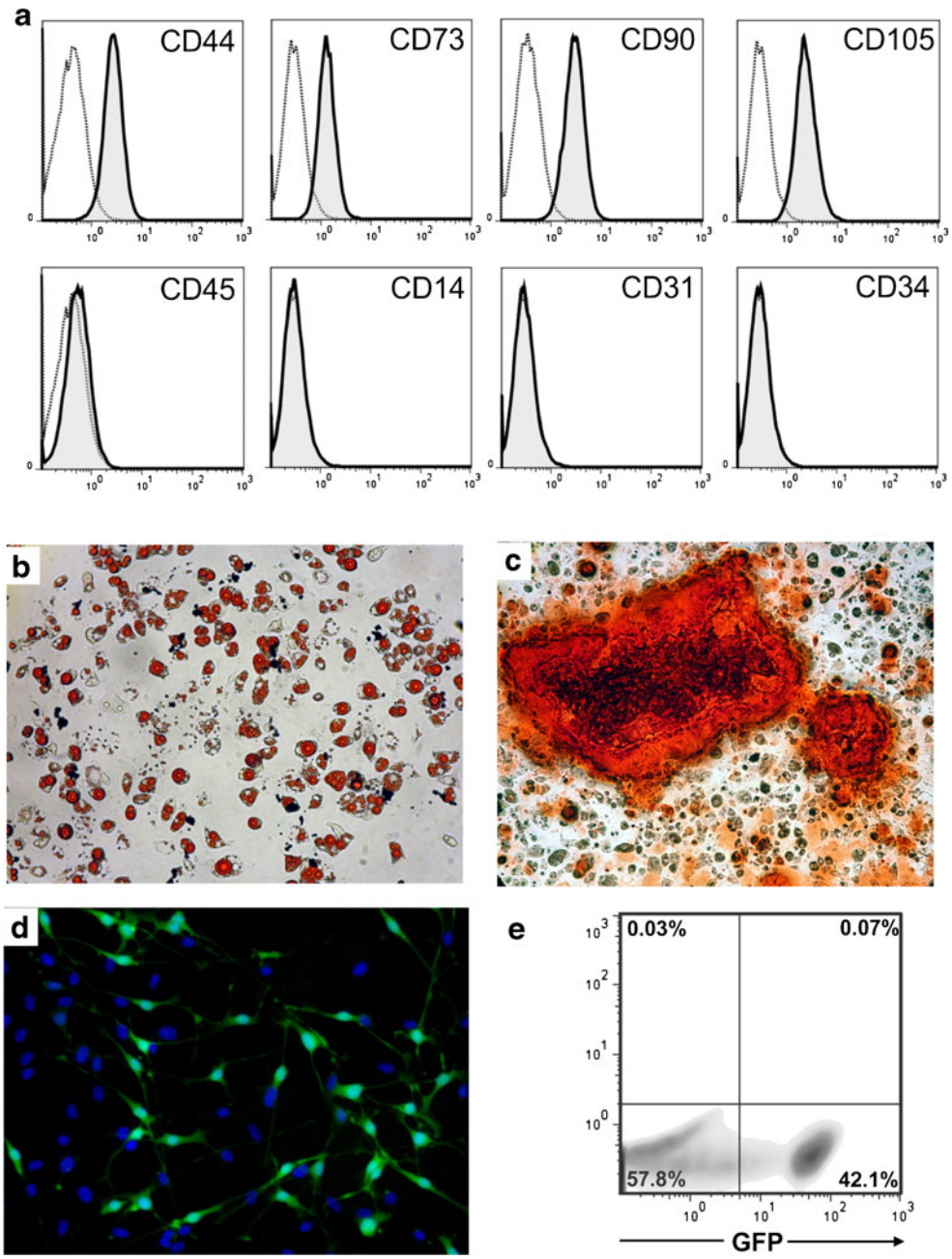

Fig. 1 Characterization of GFP-Balb/c bone marrow-derived MSCs. (**a**) Phenotypic characterization of BM-MSCs by flow cytometric analysis. GFP-Balb/c BM-MSCs express the stromal determinants CD44, CD73, CD90 and CD105, while are negative for the monocite/macrofage (CD14), endothelial (CD31 and CD34) and hematopoietic (CD45) markers. Solid *gray* histograms represent cells stained with fluorescent antibodies. Isotype-matched controls are overlaid in a *dotted black line* on each histogram. (**b**) GFP-Balb/c BM-MSCs derived adipocytes. Cells were stained with Oil Red O at day 15 to visualize lipid droplet accumulation. Original magnification: ×200. (**c**) GFP-Balb/c BM-MSCs osteogenic differentiation. Cells were stained with Alizarin Red S after 21 days of osteogenic induction to visualize mineralized bone matrix. Original magnification: ×200. (**d**) Fluorescent micrograph of BM-MSCs to determine GFP expression (*green*). Nuclei were stained with DAPI (*blue*). Original magnification: ×200. (**e**) Representative flow cytometry analysis of GFP expression in GFP-Balb/c BM-MSCs

stromal determinants, CD44, CD73, CD90, and CD105 but were negative for CD45, CD14, CD34 and CD31. We showed that BM-MSCs could be differentiated into adipocytes and osteogenic cells, consistent with established criteria for MSCs (Fig. 1b–c) [30]. GFP positive cells were present at a frequency of 48±7 % by flow cytometry (n =4) (Fig. 1d–e).

Cardiac Functional Assessment and Infarct Size After MSC Infusion

At 21 days post-MI, mice were compared first, for changes in morphological and functional cardiac parameters in vivo by echocardiography and hemodynamic measurements, and second, following sacrifice, for changes in cardiac dimensions by morphometric analysis. On the basis of postmortem examination at 21 days, all the ischemia-reperfused and fixed LAD-ligated mice developed LV transmural infarction with subsequent ventricular wall thinning and scar formation, in contrast to the normal myocardium from sham-operated animals (Table S1 and S3; Figure S2). The infarct sizes for the groups of mice studied were 52.6±7.5 % (MI+saline) and 49.8± 5.2 % (MI+MSCs) for the MI model (Table S2), and 42.7± 5.7 % (I/R+saline) and 40.1±4.8 % (I/R+MSCs) for the I/R model (Table S4). In all cases, we observed an extensive apical involvement which were not significantly different from each other. Morphometric analysis of postmortem hearts confirmed that all LAD-ligated mice developed hypertrophy on the basis of direct visualization of the hypertrophy of the non-infarcted LV muscle (Figure S2) and increase in LV/BW mass (Table S1 and S3). LAD ligation had no effect on the right ventricle weight/BW in any group of mice (Table S1). Interestingly, the lung weight/BW ratio was increased in the LAD-ligated groups. All LAD-ligated and sham-operated mice had similar total body weights (BW) (Table S1 and S3).

Of all the functional parameters examined, a significant difference was observed for LVEDP which was increased (indicative of decreased cardiac function) in mice that underwent infarction and/or ischemia-reperfusion and received saline compared with sham-operated mice (Fig. 2). Hemodynamic monitoring indicated that all mice receiving BM-MSCs had improved cardiac function. LVEDP was similar to values in sham–operated mice and significantly better than for mice with experimentally induced AMI receiving intravenous saline (Fig. 2). However, other parameters of cardiac function were not significantly enhanced (Table S1 and S3). Echocardiography demonstrated additional differences in the LV architecture post-LAD ligation among the groups of mice with respect to septal wall thickness (SWT) and LV chamber dilatation gauged by LVIDd and LVIDs (Table S2 and S4). In all LAD-ligated mice there were significant decreases in SWT and increases in dilatation of the LV chamber, based on increased LVIDd and LVIDs in respective LAD-ligated over sham-operated mice. We also examined post-MI changes in parameters related to cardiac function including FS and EF by echocardiography. LAD-ligated mice receiving saline had reduced cardiac function as assessed by decreases in FS and EF compared to LAD-ligated mice receiving BM-MSCs which were similar to their respective sham-operated controls (Table S2 and S4).

GFP+ Cells Detected Only at Infarct Site

Indirect immunofluorescence with an anti-GFP antibody showed the presence of GFP+ cells by confocal laser microscopy only in the infarcted left ventricular myocardium of mice that underwent ischemia-reperfusion and received MSCs (Fig. 3), but not in mice that underwent AMI alone.

Cellularity of the infarct zone assessed by propidium iodide (PI) staining showed the relative paucity of cells, even in those animals that received BM-MSCs (Fig. 3b). The frequency of GFP+ cells in these sections is demonstrated in Fig. 3c (from the same section as Fig. 3a). GFP+ cells were not detected in the infarcted myocardium of mice that received only saline (Fig. 3d). A total of 5849 GFP+ cells were enumerated in the infarct zones from animals receiving BM-MSCs, representing a 10.2 % of total cellularity. To overcome the potential limitation of immunofluorescence in giving false positive results because of autofluorescence, studies were performed with paraffin sections of infarct zones using avidin-biotin peroxidase staining. The presence of GFP+ cells was confirmed only in the infarct areas with appropriate negative and positive controls (Figure S3).

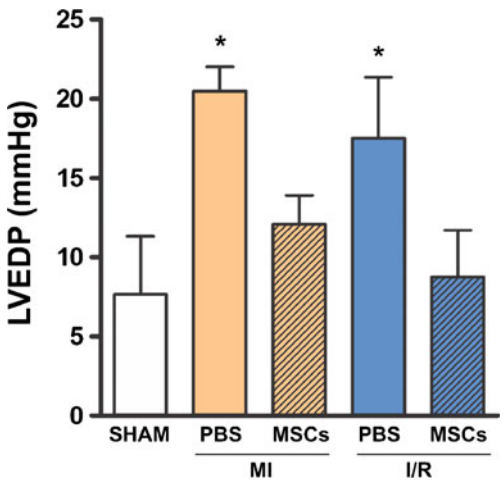

Fig. 2 The infusion of BM-MSCs improves cardiac function after MI or isquemia-reperfusion (I/R). LVEDP in 12-wk-old Balb/c mice that underwent ischemia-reperfusion LAD ligation (I/R) or LAD ligation alone (MI) followed by infusion of saline or BM-MSCs and age-matched sham-operated controls 21 days later. Bars are the mean + SD of LVEDP (mm Hg) *P <0.05 versus sham operated group, n =5–6/group

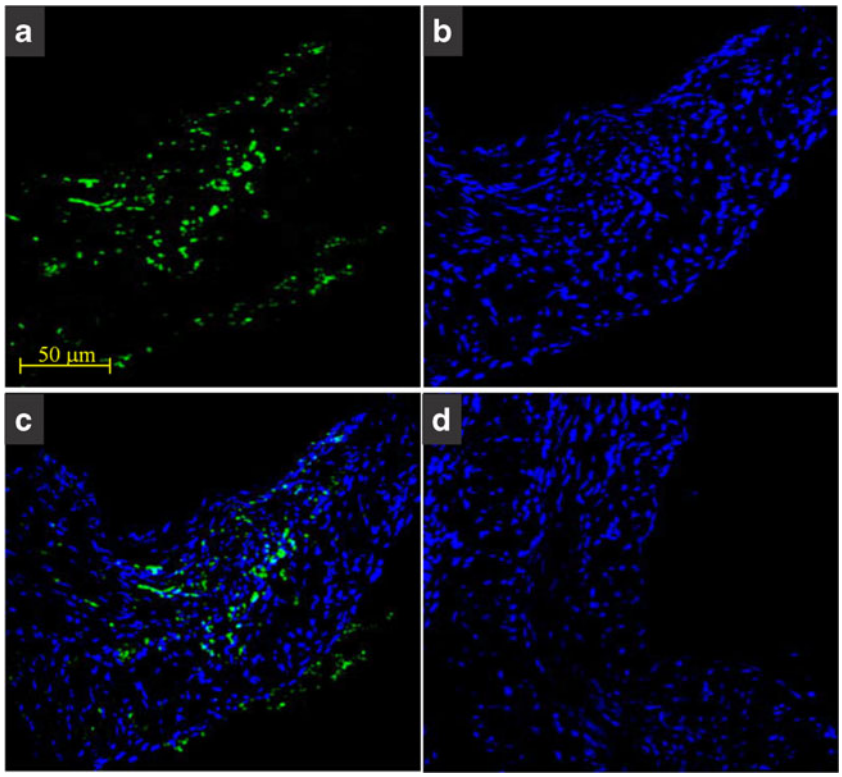

Fig. 3 GFP positive donor cells lodge in the ischemic myocardium in the I/R model. Propidium iodide (PI) staining of fixed frozen section of the I/R Balb/c myocardium 21 days after IV infusion of BM-MSCs from GFP-Balb/c. Photomicrographs were taken at the same time and in the same area using confocal laser microscopy. (**a**) Indirect immunostaining with anti-GFP and a second antibody linked with FITC, positive cells are *green*. (**b**) Propidium iodide staining of cell nuclei (*blue*) with Cy5 filter. (**c**) Merge. (**d**) PI staining of section of ischemic myocardium from saline infused control. Original magnification: ×200

Characterization of GFP+ Cells at Infarct Site

GFP+ cells were analyzed for the presence of cardiac determinants with specific antibodies against troponin T and myosin heavy chain. Troponin T, a subunit of troponin, which, together with tropomyosin, regulates cardiac muscle contraction, is expressed by mature cardiomyocyes. MF20, an anti-sarcomeric antibody, binds myosin heavy chain in embryonic, neonatal and adult cardiomyocytes. Sections were also analyzed for CD45R, CD11b, and Gr-1 (Ly-6G).

Enumeration of all the sections showed that 78 % of GFP+ cells lodging only in ischemic myocardium co-expressed troponin T (Fig. 4). Moreover, we found that many of the GFP+ cells also expressed myosin heavy chain (Fig. 5b1–5). These data demonstrate that most donor BM-MSCs had acquired at least one cardiac marker. On the other hand, 67 % of GFP+ cells co-expressed collagen type IV, indicating retention of at least one stromal cell characteristic in most donor cells (Fig. 5a1–5). The expression of other stromal markers, such as laminin and vimentin, showed similar results (Figure S4). GFP+ cells were negative for CD45 (Fig. 5c1–4), CD11b and Gr-1 (data not shown), demonstrating that the marked donor cells were non-hematopoietic in origin.

Analysis of the 5849 GFP+ cells identified in ischemic areas showed that 63.4 % (±7.5 % SD) of the donor cells

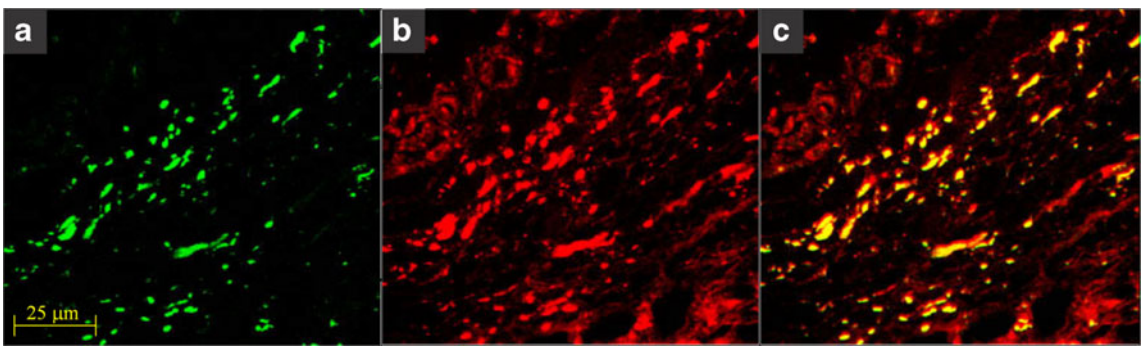

Fig. 4 GFP positive donor cells express cardiac specific Troponin T after lodgment in the MI area. Troponin T staining of frozen sections of myocardium 21 days after IV infusion of GFP-Balb/c BM-MSCs. Photomicrographs were taken at the same time and in same area using confocal laser microscopy. (**a**) Indirect immunostaining for GFP expression; GFP positive cells are *green*. (**b**) Indirect immunostaining for Troponin T; positive cells are *red*. (**c**) Merge; double positive cells are *yellow*. Original magnification: ×400

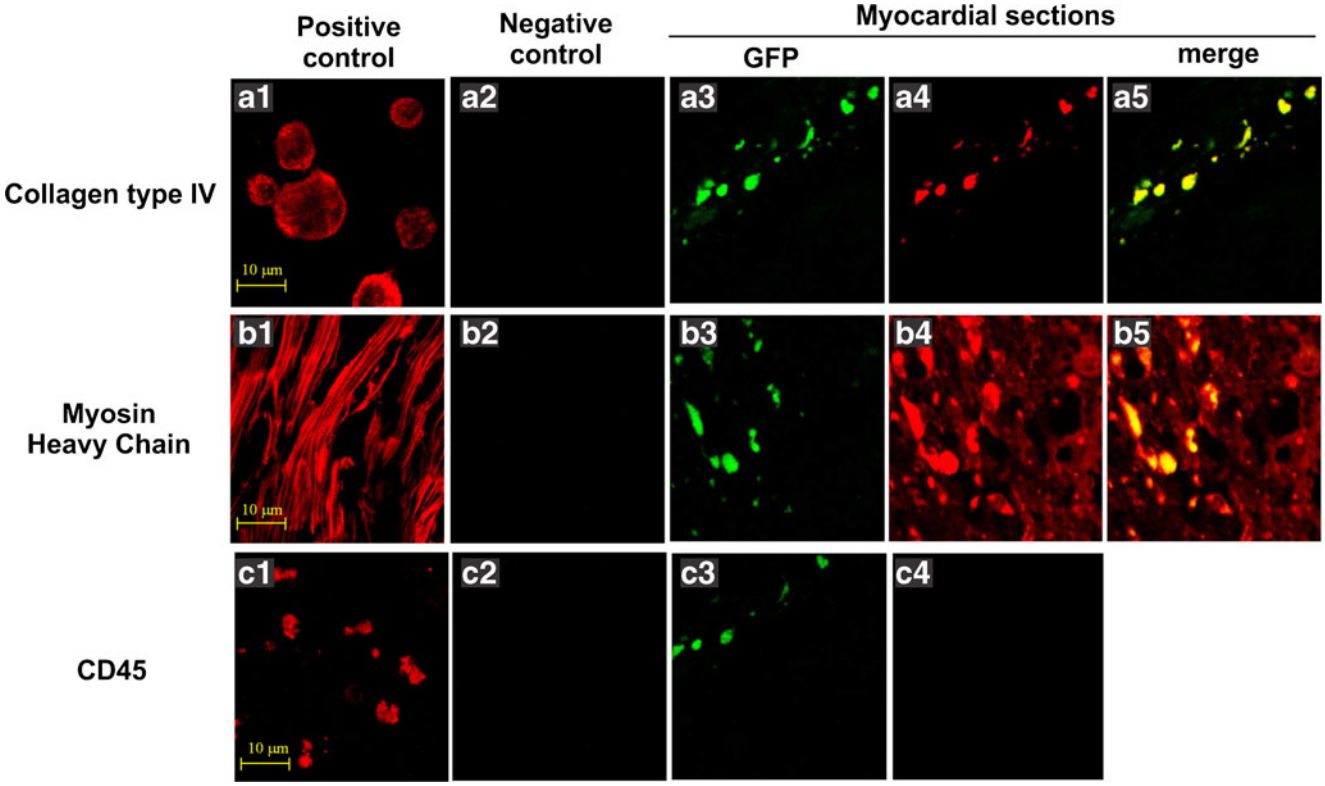

Fig. 5 Myocardial section stained for Collagen IV, myosin heavy chain, and CD45R using confocal microscopy. Sections from I/R Balb/c mice 21 days after receiving GFP-Balb/c BM-MSC. (**a1**–**5**) Collagen type IV positive cells are red. (**a1**) BM-MSCs (positive control). (**a2**) Section from wild-type Balb/c adult mice (negative control). (**a3**–**5**) Double staining of GFP and Collagen type IV. (**a3**) GFP positive cells (*green*). (**a4**) Collagen type IV positive cells (*red*). (**a5**) Merge; double positive cells are *yellow*. (**b1**–**5**) Myosin heavy chain (MHC) positive cells are *red*. (**b1**) Section of wild-type myocardium (positive control). (**b2**) MSCs (negative control). (**b3**–**5**) Myocardium from experimental animals. Double staining of GFP and myosin heavy chain. (**b3**) GFP positive cells (*green*). (**b4**) MHC positive cells (*red*). (**b5**) merge; double positive cells are *yellow*. (**c1**–**4**) CD45R positive cells are *red*. (**c1**) Mouse bone marrow cells (positive control). (**c2**) MSCs (negative control). (**c3**) GFP positive cells (*green*). (**c4**) Staining for CD45R. Original magnification: ×1000

expressed both troponin T and collagen type IV while 61.6 % (±10.2%SD) were positive with MF20 (myosin heavy chain) and co-expressed collagen type IV. These results indicate that the predominant donor cell type retained at least some of the characteristics of both MSC and cardiomyocytes (Fig. 6). However, we also found that a minor proportion of donor GFP+ cells expressed cardiac markers in the absence of stromal markers: 15.1 % (±5.1%SD) were troponin T(+) collagen type IV(-) and 25.2 % (±8.9 % SD) were myosin heavy chain positive and collagen type IV(-) (Fig. 6b). In Fig. 6a panel 4, the population of GFP+, troponin T(+) and collagen type IV(-) cells appear yellow. These data indicate that 1.6 to 2.7 % of the total cells present in the ischemic myocardium were donor derived, expressed cardiac markers and lacked a stromal marker. Interestingly, an even lower frequency of GFP+ cells retained a stromal marker without co-expressing the cardiac determinants, troponin T (4.0±13.5 %) or myosin heavy chain (12.6±13.5 %) (Fig. 6b).

Finally, we investigated the expression of the pluripotency transcription factor OCT4 in MSCs. Balb/c BM-MSCs expressed OCT4 mRNA and protein, as assessed by RT-PCR and Western-Blotting, respectively (Fig. 7a and b). Immunocytochemistry analysis indicated that 77.8±7 % of the nuclei were positive for OCT4 staining prior to infusion (Fig. 7c). Enumeration of the heart sections showed that only 4.6±5 % of the GFP+ cells identified in ischemic areas were positive for OCT4 staining ($p<0.001$ when compared with pre-infusion)(Fig. 7d). These results indicate that lodged BM-MSCs acquired a more differentiated phenotype with an associated down-regulation of this transcription factor.

Discussion

We previously showed that cells co-expressing cardiac and stromal determinants arise from murine BM-MSCs co-cultured with rat embryonic cardiomyocytes independently of cell fusion [18]. Here, we investigated whether similar cells were present after infusion of BM-MSCs in an experimental model of AMI, and determined the frequency and extent of reprogramming of these cells in injured tissue.

Although it is now generally accepted that improvement in hemodynamic function after treatment with MSCs in experimental AMI models is attributable to paracrine effects [31] as

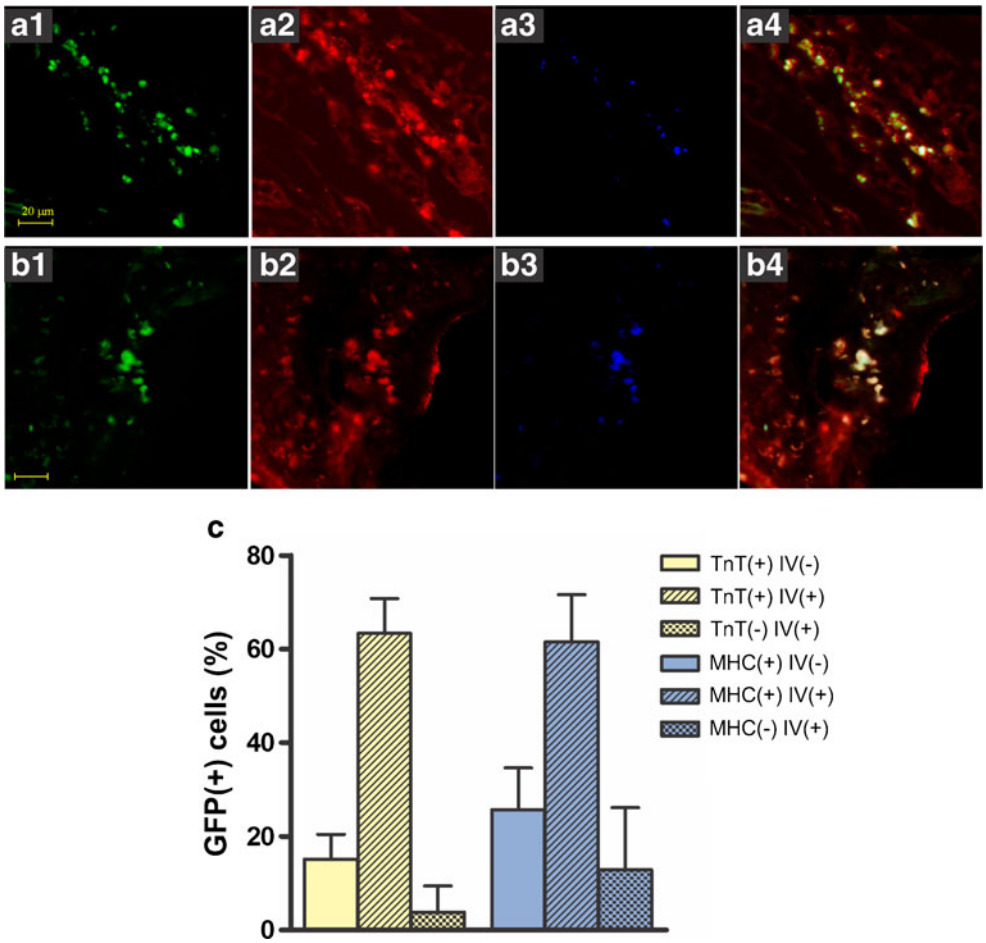

Fig. 6 GFP positive donor cells co-express both cardiac specific Troponin T or myosin heavy chain and Collagen type IV in MI area. (**a1**) Indirect immunostaining for GFP (*green*). (**a2**) Indirect immunostaining for Troponin T (*red*). (**a3**) Indirect immunostaining for collagen type IV (*blue*). (**a4**) Merge. Original magnification: ×630. (**B1**) Indirect immunostaining for GFP (*green*). (**b2**) Indirect immunostaining for myosin heavy chain (*red*). (**B3**) Indirect immunostaining for collagen type IV (*blue*). (**b4**) Merge. Original magnification: ×630. (**c**) Frequency of GFP(+) donor cells expressing the cardiac determinants troponin T (TnT) or myosin heavy chain (MHC) with or without co-expressing the stromal marker collagen type IV (IV) in 30 sections of ischemic myocardium from 5 animals receiving BM-MSCs ($n = 5849$). Bars represent the mean + SD

well as to a macrophage-mediated anti-inflammatory response, as we previously showed [11], the nature and importance of donor cells lodged at the injury site remain to be determined. While several studies a decade ago had claimed to identify cardiomyocytes derived from BM-derived donor cells [7, 32–35] and ushered in an era of clinical investigation [36] more definitive pre-clinical work failed to confirm these observations [37, 38]. Indeed, most of the more recent studies claim only the transient presence of donor cells at injury sites, casting doubt on the importance of the cells at those locations to mediate tissue regeneration and provide additional indirect evidence for the primacy of allocrine or paracrine effects [11, 14, 16]. Our observation of non-fused cells co-expressing stromal and cardiomyocyte markers in vitro [18] led us to investigate the presence of a similar cell type in vivo.

We believed that it was important to avoid the technical pitfalls encountered in earlier studies, including false positive results due to autofluorescence as well as differences in potentially important variables in the experimental methodology, including fixed versus ischemia/reperfusion models of AMI, the means of marking and identifying donor cells, the timing of cell administration, the cell type administered, the method of cell preparation and the cell dose given. The stromal cell population was intrinsically marked (obtained from GFP-Balb/c mice) and well characterized prior to infusion. False positive results from autofluorescence were eliminated by the use of multiple chromophore-antibody combinations to confirm the expression of GFP-marked cells. In addition, avidin-biotin peroxidase methodology unequivocally demonstrated the presence of donor GFP positive cells in the injured myocardium. Finally, we employed the ischemia/reperfusion model to induce AMI as a more accurate reflection of the pathological process in humans.

We showed that GFP-marked BM-MSCs lodged only at the site of injured myocardium in the ischemia-reperfusion model: approximately 10 % of the cells at the infarct site were of donor origin. Recent reports have shown that infused human MSCs can enhance cardiac tissue repair without significant engraftment [11, 14]. Of note, these studies administered higher cell doses and demonstrated that the benefit on cardiac function was not related to the presence of cells at the infarct area but to the release of anti-inflammatory cytokines by MSCs. Previous reports of intramyocardial retention of MSCs [5, 7, 8], did not investigate the phenotypic heterogeneity of lodged donor cells. It is of interest that our data demonstrated that 15–25 % of the lodged marked donor cells

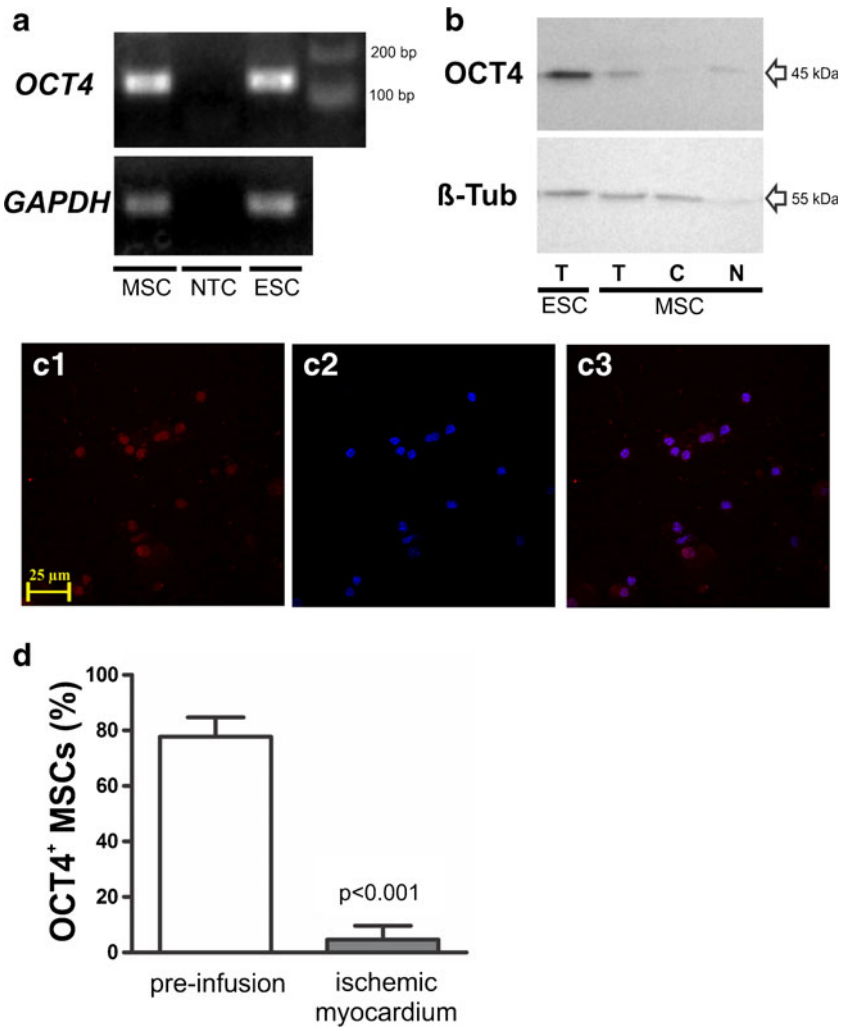

Fig. 7 GFP-Balb/c MSCs lose the expression of the pluripotency factor OCT4 after lodgment in the MI area. (**a**) RT-PCR analysis. Positive control, ESC; no template control, NTC. GAPDH was used as an internal control. (**b**) OCT4 protein expression assessed by Western Blotting in total protein extracts (T), cytoplasmic fraction (C) and nuclear fraction (N). Positive control, ESC. β-Tubulin (β-Tub) immunoblotting was performed as an internal control. (**c**1) Indirect immunostaining for OCT4 expression (*red*). (**c**2) Total nuclei were stained with DAPI (*blue*). (**c**3) Merge. Original magnification: ×400. (**d**) Percentage of OCT4 positive GFP-Balb/c BM-MSCs before the infusion and after lodgment in the ischemic area for 21 d. Bars represent the mean + SD ($n=5$)

expressed cardiomyocyte markers and lacked all the MSC determinants assayed. Most of the lodged donor cells (63 %) however, expressed an immunophenotype that co-expressed stromal and cardiomyocyte markers, confirming in vivo our in vitro observation. In our in vitro studies the cells of MSC origin exhibiting cardiac-specific gene expression neither generated spontaneous or evoked action potentials nor produced ionic currents typical of cardiomyocytes, indicating that they were not functional cardiomyocytes [18].

These data infer the existence of a predominant cell type that only partially differentiates in vivo in response to signals at the site of injury and suggests that the acquisition of a more differentiated cardiomyocyte phenotype is less frequent but can occur in up to 25 % of the donor cells. To obtain further insight into possible mechanisms we studied expression and modulation of the stemness transcription factor, OCT4. It is well-known that OCT4 plays an important role in self-renewal and cell fate determination in human and mouse embryonic stem cells (ESC) [39, 40]. In addition, several reports have shown that OCT4 inhibits tissue-specific genes and is down-regulated upon differentiation of ESCs [41, 42]. Similar regulatory mechanisms for OCT4 have been found in human MSCs [43]. Here, we demonstrated that Balb/c BM-MSCs constitutively expressed this pluripotency transcription factor, but lost expression after lodgment in the infarct area. These results indicate that lodged MSCs may undergo growth arrest and a program of differentiation, supporting the finding that most marked cells co-expressed stromal and cardiac determinants and some donor cells expressed only cardiac determinants and lacked the stromal markers tested. Future experiments are required to delineate the importance of OCT4 in mediating cardiac reprogramming of MSCs.

Although we were not able to determine the frequency of cell fusion between MSCs and cardiomyocytes for technical reasons in our in vivo studies, we believe that the highest levels likely to be obtained for this phenomenon would be between embryonic and other cells, as reported in the literature and in our own in vitro experiments [18, 44]. In the co-culture studies of rat embryonic cardiomyocytes and adult mouse BM-MSCs, we observed a cell fusion frequency of 0.7 % which could

not account for the 6.3 % cells co-expressing cardiac and stromal markers [18]. In contrast, in our in vivo experiments the potential cell fusion partners were adult cells, including the predominantly not-mitotic resident cardiomyocytes, hence cell fusion would be extremely unlikely to explain the 63 % of donor cells co-expressing stromal and cardiac markers. In this context, Noiseux et al. [16] demonstrated, using an appropriate study design to quantify fused cells, that cellular fusion between MSC and recipient cardiomyocytes is an extremely low event and occurs within the infarct border zone in a mouse model of AMI.

Taken together, our results extend the work of others who demonstrated the expression of cardiac proteins in extrinsically marked MSCs [5, 7, 8]. We contend that the low levels of donor cells at the injury site expressing cardiomyocyte markers but lacking MSC determinants are unlikely to account for the improvement, albeit limited, in cardiac function. While increasing evidence favors MSC-mediated improvement of cardiac function by release of a wide array of soluble growth factors and cytokines, the contribution of the different sub-populations of MSCs detected at the injury site remains unknown. Further studies are required to determine the contributions, especially of the predominant cell population that co-express stromal and cardiac markers, but also of cells of MSC origin that have acquired cardiac markers and lost MSC determinants as well as the unmodified MSCs. We speculate that ischemic tissue serves as a microenvironment for MSCs to undergo cardiomyocyte reprogramming. Factors determining the extent of that reprogramming, as well as the cytokines expression profiles of the different MSC subpopulations themselves, may be important in better understanding cardiac regeneration. It may then be possible to identify the cell types best able to mediate this process.

Acknowledgments We are grateful to Huijie Xiang, University Health Network for outstanding technical assistance, to Qi-Long Yi (Biostatistics Department, Princess Margaret Hospital/Ontario Cancer Institute) for assistance in statistical analysis and to Ye Yang, Department of Pathology, University Health Network for technical assistance in preparation of histological sections. A.K holds the Gloria and Seymour Epstein Chair in Cell Therapy and Transplantation at the University Health Network and the University of Toronto.

Author Contributions Conceived and designed the experiments: GY, JNT, AK. Performed the experiments: GY, JNT, JFD, XHW, AP. Analyzed the data: GY, JNT. Contributed reagents/materials/analysis tools: SV, TGP, AK. Wrote the paper: GY, JNT, SV, AK.

Conflict of Interest The authors declare that they have no competing interests.

Funding This work was supported by the Orsino Translational Research Laboratory, PMH. The funders had no role in study design, data collection and analysis, decision to publish, or preparation of the manuscript.

References

1. Lloyd-Jones, D., Adams, R., Carnethon, M., et al. (2009). Heart disease and stroke statistics–2009 update: a report from the American Heart Association Statistics Committee and Stroke Statistics Subcommittee. *Circulation, 119*, 480–486.
2. Hare, J. M., Fishman, J. E., Gerstenblith, G., et al. (2012). Comparison of allogeneic vs autologous bone marrow–derived mesenchymal stem cells delivered by transendocardial injection in patients with ischemic cardiomyopathy: the POSEIDON randomized trial. *JAMA, 308*, 2369–2379.
3. Psaltis, P. J., Zannettino, A. C., Worthley, S. G., & Gronthos, S. (2008). Concise review: mesenchymal stromal cells: potential for cardiovascular repair. *Stem Cells, 26*, 2201–2210.
4. Li, X., Yu, X., Lin, Q., et al. (2007). Bone marrow mesenchymal stem cells differentiate into functional cardiac phenotypes by cardiac microenvironment. *Journal of Molecular and Cellular Cardiology, 42*, 295–303.
5. Makino, S., Fukuda, K., Miyoshi, S., et al. (1999). Cardiomyocytes can be generated from marrow stromal cells in vitro. *Journal of Clinical Investigation, 103*, 697–705.
6. Shim, W. S., Jiang, S., Wong, P., et al. (2004). Ex vivo differentiation of human adult bone marrow stem cells into cardiomyocyte-like cells. *Biochemical and Biophysical Research Communications, 324*, 481–488.
7. Toma, C., Pittenger, M. F., Cahill, K. S., Byrne, B. J., & Kessler, P. D. (2002). Human mesenchymal stem cells differentiate to a cardiomyocyte phenotype in the adult murine heart. *Circulation, 105*, 93–98.
8. Tomita, S., Li, R. K., Weisel, R. D., et al. (1999). Autologous transplantation of bone marrow cells improves damaged heart function. *Circulation, 100*, II247–II256.
9. Keating, A. (2005). Bone marrow cells for cardiac repair. *Biology of Blood and Marrow Transplantation, 11*, 2–6.
10. Hale, S. L., Dai, W., Dow, J. S., & Kloner, R. A. (2008). Mesenchymal stem cell administration at coronary artery reperfusion in the rat by two delivery routes: a quantitative assessment. *Life Sciences, 83*, 511–515.
11. Dayan, V., Yannarelli, G., Billia, F., et al. (2011). Mesenchymal stromal cells mediate a switch to alternatively activated monocytes/macrophages after acute myocardial infarction. *Basic Research in Cardiology, 106*, 1299–1310.
12. Fazel, S., Cimini, M., Chen, L., et al. (2006). Cardioprotective c-kit+ cells are from the bone marrow and regulate the myocardial balance of angiogenic cytokines. *Journal of Clinical Investigation, 116*, 1865–1877.
13. Gallo, M. P., Ramella, R., Alloatti, G., et al. (2007). Limited plasticity of mesenchymal stem cells cocultured with adult cardiomyocytes. *Journal of Cellular Biochemistry, 100*, 86–99.
14. Lee, R. H., Pulin, A. A., Seo, M. J., et al. (2009). Intravenous hMSCs improve myocardial infarction in mice because cells embolized in lung are activated to secrete the anti-inflammatory protein TSG-6. *Cell Stem Cell, 5*, 54–63.
15. Mirotsou, M., Zhang, Z., Deb, A., et al. (2007). Secreted frizzled related protein 2 (Sfrp2) is the key Akt-mesenchymal stem cell-released paracrine factor mediating myocardial survival and repair. *Proceedings of the National Academy of Sciences of the United States of America, 104*, 1643–1648.
16. Noiseux, N., Gnecchi, M., Lopez-Ilasaca, M., et al. (2006). Mesenchymal stem cells overexpressing Akt dramatically repair infarcted myocardium and improve cardiac function despite infrequent cellular fusion or differentiation. *Molecular Therapy, 14*, 840–850.
17. Yannarelli, G., Dayan, V., Pacienza, N., et al. (2013). Human umbilical cord perivascular cells exhibit enhanced cardiomyocyte reprogramming and cardiac function after experimental acute myocardial infarction. *Cell Transplantation, 22*, 1651–1666. doi:10.3727/096368912X657675.

18. Rose, R. A., Jiang, H., Wang, X., et al. (2008). Bone marrow-derived mesenchymal stromal cells express cardiac-specific markers, retain the stromal phenotype, and do not become functional cardiomyocytes in vitro. *Stem Cells, 26*, 2884–2892.
19. Kasper, G., Dankert, N., Tuischer, J., et al. (2007). Mesenchymal stem cells regulate angiogenesis according to their mechanical environment. *Stem Cells, 25*, 903–910.
20. Bartunek, J., Croissant, J. D., Wijns, W., et al. (2007). Pretreatment of adult bone marrow mesenchymal stem cells with cardiomyogenic growth factors and repair of the chronically infarcted myocardium. *American Journal of Physiology - Heart and Circulatory Physiology, 292*, H1095–H1104.
21. Behfar, A., Yamada, S., Crespo-Diaz, R., et al. (2010). Guided cardiopoiesis enhances therapeutic benefit of bone marrow human mesenchymal stem cells in chronic myocardial infarction. *Journal of the American College of Cardiology, 56*, 721–734.
22. Okura, H., Matsuyama, A., Lee, C. M., et al. (2010). Cardiomyoblast-like cells differentiated from human adipose tissue-derived mesenchymal stem cells improve left ventricular dysfunction and survival in a rat myocardial infarction model. *Tissue Engineering. Part C, Methods, 16*, 417–425.
23. Potapova, I. A., Doronin, S. V., Kelly, D. J., et al. (2008). Enhanced recovery of mechanical function in the canine heart by seeding an extracellular matrix patch with mesenchymal stem cells committed to a cardiac lineage. *American Journal of Physiology - Heart and Circulatory Physiology, 295*, H2257–H2263.
24. Yoon, J., Min, B. G., Kim, Y. H., Shim, W. J., Ro, Y. M., & Lim, D. S. (2005). Differentiation, engraftment and functional effects of pretreated mesenchymal stem cells in a rat myocardial infarct model. *Acta Cardiologica, 60*, 277–284.
25. Bubnic, S. J., Wang, X. H., Clark, B. R., & Keating, A. (2002). W/Wv marrow stromal cells engraft and enhance early erythropoietic progenitors in unconditioned Sl/Sld murine recipients. *Bone Marrow Transplantation, 30*, 867–872.
26. Desjardins, J. F., Pourdjabbar, A., Quan, A., et al. (2009). Lack of S100A1 in mice confers a gender-dependent hypertensive phenotype and increased mortality after myocardial infarction. *American Journal of Physiology - Heart and Circulatory Physiology, 296*, H1457–H1465.
27. Tsoporis, J. N., Marks, A., Haddad, A., Dawood, F., Liu, P. P., & Parker, T. G. (2005). S100B expression modulates left ventricular remodeling after myocardial infarction in mice. *Circulation, 111*, 598–606.
28. Liedtke, S., Enczmann, J., Waclawczyk, S., Wernet, P., & Kögler, G. (2007). Oct4 and its pseudogenes confuse stem cell research. *Cell Stem Cell, 1*, 364–366.
29. Maniatis, T., Sambrook, J., & Fritsch, E. F. (1989). *Molecular Cloning: A Laboratory Manual* (2nd ed., pp. 18.38–18.39). New York: Cold Spring Harbour Laboratory Press.
30. Dominici, M., Le Blanc, K., Mueller, I., et al. (2006). Minimal criteria for defining multipotent mesenchymal stromal cells. The International Society for Cellular Therapy position statement. *Cytotherapy, 8*, 315–317.
31. Keating, A. (2012). Mesenchymal stromal cells: new directions. *Cell Stem Cell, 10*, 709–716.
32. Jackson, K. A., Majka, S. M., Wang, H., et al. (2001). Regeneration of ischemic cardiac muscle and vascular endothelium by adult stem cells. *Journal of Clinical Investigation, 107*, 1395–1402.
33. Orlic, D., Kajstura, J., Chimenti, S., et al. (2001). Bone marrow cells regenerate infarcted myocardium. *Nature, 410*, 701–705.
34. Orlic, D., Kajstura, J., Chimenti, S., et al. (2001). Mobilized bone marrow cells repair the infarcted heart, improving function and survival. *Proceedings of the National Academy of Sciences of the United States of America, 98*, 10344–10349.
35. Yeh, E. T., Zhang, S., Wu, H. D., Körbling, M., Willerson, J. T., & Estrov, Z. (2003). Transdifferentiation of human peripheral blood CD34+-enriched cell population into cardiomyocytes, endothelial cells, and smooth muscle cells in vivo. *Circulation, 108*, 2070–2073.
36. Martin-Rendon, E., Brunskill, S. J., Hyde, C. J., Stanworth, S. J., Mathur, A., & Watt, S. M. (2008). Autologous bone marrow stem cells to treat acute myocardial infarction: a systematic review. *European Heart Journal, 29*, 1807–1818.
37. Balsam, L. B., Wagers, A. J., Christensen, J. L., Kofidis, T., Weissman, I. L., & Robbins, R. C. (2004). Haematopoietic stem cells adopt mature haematopoietic fates in ischaemic myocardium. *Nature, 428*, 668–673.
38. Murry, C. E., Soonpaa, M. H., Reinecke, H., et al. (2004). Haematopoietic stem cells do not transdifferentiate into cardiac myocytes in myocardial infarcts. *Nature, 428*, 664–668.
39. Ohtsuka, S., & Dalton, S. (2008). Molecular and biological properties of pluripotent embryonic stem cells. *Gene Therapy, 15*, 74–81.
40. Silva, J., & Smith, A. (2008). Capturing pluripotency. *Cell, 132*, 532–536.
41. Camara-Clayette, V., Le Pesteur, F., Vainchenker, W., & Sainteny, F. (2006). Quantitative Oct4 overproduction in mouse embryonic stem cells results in prolonged mesoderm commitment during hematopoietic differentiation in vitro. *Stem Cells, 24*, 1937–1945.
42. Niwa, H., Miyazaki, J., & Smith, A. G. (2000). Quantitative expression of Oct-3/4 defines differentiation, dedifferentiation or self-renewal of ES cells. *Nature Genetics, 24*, 372–376.
43. Greco, S. J., Liu, K., & Rameshwar, P. (2007). Functional similarities among genes regulated by OCT4 in human mesenchymal and embryonic stem cells. *Stem Cells, 25*, 3143–3154.
44. Ramkisoensing, A. A., Pijnappels, D. A., Askar, S. F., et al. (2011). Human embryonic and fetal mesenchymal stem cells differentiate toward three different cardiac lineages in contrast to their adult counterparts. *PLoS One, 6*, e24164.